Direct Kinetic Evidence for Half-Of-The-Sites Reactivity in the E1 Component of the Human Pyruvate Dehydrogenase Multienzyme Complex through Alternating Sites Cofactor Activation†

Franziska Seifert,‡ Ralph Golbik,‡ Johanna Brauer,‡ Hauke Lilie,§ Kathrin Schröder-Tittmann,§ Erik Hinze,‡ Lioubov G. Korotchkina,|| Mulchand S. Patel,|| and Kai Tittmann*,‡

Institut für Biochemie and Institut für Biotechnologie, Martin-Luther-Universität Halle-Wittenberg, Kurt-Mothes-Strasse 3, D-06120 Halle/Saale, Germany, and State University of New York, Buffalo, New York 14260

Received August 4, 2006

ABSTRACT: Recent kinetic and structural studies on various thiamin-dependent enzymes, including the bacterial E1 component of the pyruvate dehydrogenase complex (PDHc), suggested an active center communication between the cofactors in these multimeric enzymes. This regulatory mode has been inferred from the dissymmetry of active sites in proteolytic patterns and X-ray structures and from a complex macroscopic kinetic behavior not being consistent with independently working active sites. Here, direct microscopic kinetic evidence for this hypothesis is presented for the $\alpha_2\beta_2$-type E1 component of the human pyruvate dehydrogenase complex. Only one of the two thiamin molecules bound to the two active sites is in a chemically activated state exhibiting an apparent C2 ionization rate constant of approximately 50 s^{-1} at pH 7.6 and 30 °C, whereas the thiamin in the "inactive site" ionizes with a rate that is at least 3 orders of magnitude smaller. The chemical nonequivalence is also exhibited in the ability to bind the substrate analogue methyl acetylphosphonate and in the catalytic turnover of the substrate pyruvate in the E1-only reaction. In the activated active site, pyruvate is rapidly bound and decarboxylated with apparent forward rate constants of covalent pyruvate binding of 2 s^{-1} and decarboxylation of the formed 2-lactyl-thiamin intermediate of 5 s^{-1}. In the dormant site, these steps are as slow as 0.03 s^{-1}. Under the conditions that were used, only the heterotetramer can be detected by analytical ultracentrifugation, thus ruling out the possibility that multiple oligomeric species with different reactivities cause the observed kinetic effects. The results are consistent with the recently suggested model of an active site synchronization in PDHc-E1 via a proton wire that keeps the two active sites in an alternating activation state [Frank, R. A., et al. (2004) *Science 306*, 872]. Kinetic studies on the related thiamin enzymes transketolase, pyruvate oxidase, and bacterial pyruvate decarboxylase are not consistent with a chemical and/or functional nonequivalence of the active sites as observed in the E1 component of *hs*PDHc. We hypothesize that the alternating sites reaction in PDHc-E1 aids in the synchronized acyl transfer to the E2 component in the highly organized multienzyme complex.

The human pyruvate dehydrogenase multienzyme complex (PDHc)[1] catalyzes the oxidative decarboxylation of pyruvate to acetyl-CoA in the following overall reaction (*1*):

$$\text{pyruvate} + \text{CoA} + \text{NAD}^+ \rightarrow \text{acetyl-CoA} + \text{CO}_2 + \text{NADH} + \text{H}^+ \quad (1)$$

The components that are involved in this reaction are the thiamin diphosphate (ThDP)-dependent pyruvate dehydrogenase (E1), the dihydrolipoamide transacetylase (E2) containing covalently bound lipoyl groups, the lipoamide dehydrogenase (E3) with a tightly bound flavin, and the E3-binding protein (E3BP). In addition to these four major components, mammalian PDHc also contains pyruvate dehydrogenase kinase (PDK) and pyruvate dehydrogenase phosphatase (PDP), which serve to control the activation state of E1 by phosphorylating or dephosphorylating three serine residues (*2*−*4*).

The E1 component catalyzes the initial decarboxylation of pyruvate and the subsequent reductive acetylation of a lipoyl group covalently attached to a lysine residue in E2 (Scheme 1). After ionization of the reactive C2 of ThDP and formation of the Michaelis complex, the C2 carbanion of ThDP attacks the carbonyl carbon of the substrate pyruvate

† This work has been supported in part by Grant 0126FP/0705M (to K.T.) by the Ministry of Education Saxony-Anhalt.

* To whom correspondence should be addressed. E-mail: kai.tittmann@biochemtech.uni-halle.de. Phone: ++49-345-5524887. Fax: ++49-345-5527014.

‡ Institut für Biochemie, Martin-Luther-Universität Halle-Wittenberg.

§ Institut für Biotechnologie, Martin-Luther-Universität Halle-Wittenberg.

|| State University of New York.

[1] Abbreviations: PDHc, pyruvate dehydrogenase multienzyme complex; PDHc-E1, E1 component of PDHc; ThDP, thiamin diphosphate; LThDP, 2-lactyl-ThDP; HEThDP, 2-(1-hydroxyethyl)-ThDP; $HEThDP^-$, carbanion−enamine form of HEThDP; MAP, methyl acetylphosphonate; PLThDP, 2-phosphono-LThDP; PDC, pyruvate decarboxylase; BFD, benzoylformate decarboxylase; POX, pyruvate oxidase; TK, transketolase; IPDC, indolepyruvate decarboxylase.

10.1021/bi061582l CCC: $33.50
Published on Web 09/29/2006

Scheme 1: Mechanism of the Pyruvate Dehydrogenase Complex E1 Component

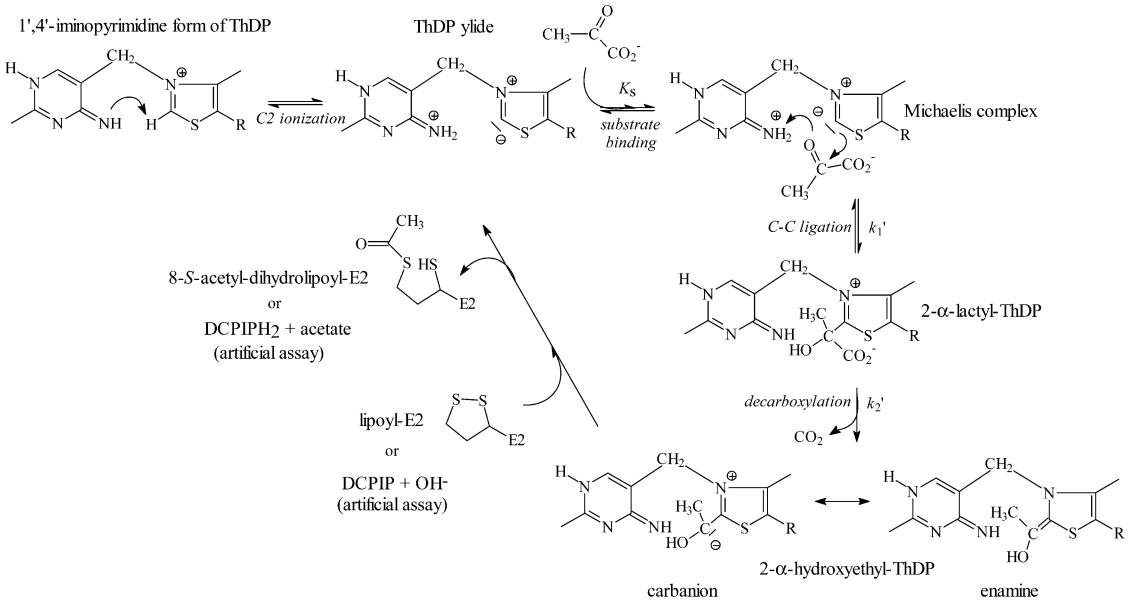

in a nucleophilic manner, yielding the tetrahedral 2-lactyl-ThDP (LThDP) intermediate (denoted as k_1'). Decarboxylation of LThDP (denoted as k_2') gives the carbanion−enamine form of 2-hydroxyethyl-ThDP (HEThDP$^-$), which in turn reduces lipoamide of the E2 component with concomitant acetyl transfer, leading to the formation of 8-*S*-acetyldihydrolipoamide-E2. The reductive acetylation step shown here to occur in a carbanion mechanism may alternatively involve transient 2-acetyl-ThDP−dihydrolipoyl-E2 intermediates in a stepwise mechanism (*5*).

The human E1 component is an $\alpha_2\beta_2$-type heterotetramer and consists of two active sites, each of which binds one ThDP and one Mg^{2+} ion. Although the X-ray structure of the human E1 component was not indicative of a structural nonequivalence of the active sites in the absence of substrates, an alternating sites flip-flop mechanism has been suggested for the catalytic turnover (*6*). Accordingly, the two active sites in *hs*PDHc-E1 were supposed to be synchronized by shuttlelike motions of one heterodimer with respect to the other heterodimer in the course of catalysis. As a consequence, both active sites would be in alternating phases of the catalytic sequence. The detailed structural analysis suggested that catalytic events in both active sites could drive the domain movements simultaneously in terms of "pull-push mechanics" (*6*). The proposed dynamic nonequivalence of the two active sites is supported by earlier kinetic studies on mammalian PDHc (*7*, *8*). Reconstitution experiments of PDHc with either ThDP or chemically synthesized HEThDP (the conjugate acid of the HEThDP enamine) revealed that only 50% of the active sites are occupied with HEThDP when compared to ThDP as demonstrated by CD spectroscopy. In view of recent studies by Jordan and co-workers (*9*, *10*), one can surmise that the observed CD signal originates from the 1′,4′-imino tautomer of the aminopyrimidinium ring of the cofactor or HEThDP$^-$ intermediate. However, the fraction of the 1′,4′-imino tautomer of bound ThDP and HEThDP in E1 need not neccessarily be equal. Therefore, these studies could not ultimately prove a half-of-the-sites mechanism.

A recent report of Perham and co-workers addressed how the active sites in E1 from *Bacillus stearothermophilus* may be synchronized (*11*, *12*). The structural nonequivalence of both active sites apparent both in the X-ray structure and in different proteolytic patterns obtained in presence of either ThDP or the carbene-like cofactor analogue 3-deaza-3-carba-ThDP (a mimic of the reactive C2 carbanion) tempted these authors to deduce that only one active site is in an activated state. On the basis of the X-ray structure, they proposed a molecular switch in terms of a proton wire via a chain of acidic side chains from one cofactor to the other. Although the structural data support the conclusions that were made, no direct kinetic evidence on a microscopic scale for a possibly different reactivity of the two cofactors had been provided. Going beyond the class of ketoacid dehydrogenases, the authors hypothesized that this active center communication might be considered a common feature of all thiamin enzymes. In line with this proposal, there have been kinetic studies on some ThDP enzymes such as yeast PDC and benzoylformate decarboxylase which are not consistent with independently working active sites (*13*).

To test whether the two active sites in human E1 exhibit a different chemical reactivity, we (i) characterized the activation state of enzyme-bound ThDP by determining the ionization rate constant of the reactive C2 using a H−D exchange technique (*14*), (ii) kinetically analyzed the E1-only reaction which encompasses all catalytic steps up to and including formation of the central carbanion−enamine intermediate (steps 1−3 in Scheme 1) by transient chemical quench−NMR studies (*15*), and (iii) examined the ability of both active sites in E1 to bind the pyruvate analogue methyl acetylphosphonate. Our results show that only one of the two cofactor molecules in the active sites is in an activated state. As a consequence of this chemical nonequivalence, only the "reactive site" in E1 catalyzes a fast pyruvate decarboxylation to yield the carbanion−enamine intermediate. These findings are consistent with the proton wire mechanism suggested by Perham and co-workers. According to this, both active sites are synchronized by a proton shuttle, which serves to reversibly transfer a proton between the active sites. In that way, deprotonation of the central enamine in the course of reductive acetylation at the

reactive site would trigger activation and substrate binding in the other active site and vice versa.

MATERIALS AND METHODS

Protein Expression and Purification. Escherichia coli M15 cells containing the pQE-9-6HE1α/E1β plasmid (*16*) were grown on a LB plate containing 100 μg/mL ampicillin and 25 μg/mL kanamycin overnight at 37 °C. A single colony from plates was used to inoculate an overnight culture of either (i) 2 × 50 mL for cell cultivation in flasks or (ii) 300 mL for cell cultivation in a fermenter (B. Braun Biotech) at 37 °C. In both cases, the overnight culture was centrifuged at 6000 rpm and 5 °C for 20 min. The pellet that was obtained was resuspended in 30 mL (flasks) or 300 mL (fermentation) of fresh LB medium containing 100 μg/mL ampicillin and 25 μg/mL kanamycin. Thereafter, cell suspensions were used to inoculate either 12 L of LB medium in flasks or, alternatively, 8 L of yeast extract in a biofermenter, each containing 100 μg/mL ampicillin and 25 μg/mL kanamycin. In the former case, cells were grown to an OD_{600} of 0.8 and the overexpression was initiated by the addition of 1 mM IPTG and 100 μg/mL thiamin. The cultures were then grown overnight at 30 °C. The cells were harvested by centrifugation at 6000 rpm for 20 min at 5 °C. The pellet (wet weight of approximately 60−70 g) was resuspended in washing buffer containing 50 mM potassium phosphate (pH 7.0), 1 mM EDTA, 1 mM DTE, and 10 mM imidazole (150−200 mL for 12 L of culture). For storage, the cell suspension was shock-frozen in liquid nitrogen and stored at −70 °C until it was used.

In the biofermenter, the culture was stirred with increasing velocity from 600 to 1500 rpm at a $p(O_2)$ of 100% and 37 °C. The rate of air flow was increased from 3 to 12 L/min. The pH was kept constant at 7.0 by addition of NH_4OH (15%). After the sample had reached an OD_{600} of 45, the temperature was decreased to 25 °C. The expression of the gene encoding *hs*PDH-E1 was initiated by addition of 1 mM IPTG and 100 μg/mL thiamin. After induction, cells were grown until an OD_{600} of 106 was reached. After centrifugation (6000 rpm for 20 min at 4 °C), the cell mass (wet weight of approximately 1340 g from 8 L of culture) was shock-frozen in liquid nitrogen and stored at −70 °C.

For purification, 60−70 g of cells was thawed on ice and resuspended in 150−200 mL of buffer containing 50 mM potassium phosphate (pH 7.0), 1 mM EDTA, 1 mM DTE, and 10 mM imidazole. In addition, DNase (5 μg/mL), $MgSO_4$ (1 mM), PMSF (1 mM), and lysozyme (1 mg/mL) were added. The suspension was stirred for 45 min at 8 °C.

Cells were then lysed by repeated passages in a French press. The cell debris was separated from the soluble fraction by ultracentrifugation (30 000 rpm for 35 min at 5 °C). Nucleic acids were precipitated using streptomycin [0.8% (w/v)] at 8 °C for 30 min. After centrifugation (30 000 rpm for 35 min at 5 °C), 300 mM KCl was added to the supernatant. The protein solution was diluted in a 1:4 mixing ratio with a buffer containing 50 mM potassium phosphate (pH 7.0), 1 mM EDTA, 1 mM DTE, and 10 mM imidazole. Thereafter, the solution was loaded onto a Ni−NTA−agarose column (25 mL) previously equilibrated with 100 mL of 50 mM potassium phosphate (pH 7.0), 300 mM KCl, and 200 mM imidazole (buffer B) or 100 mL of 50 mM potassium phosphate (pH 7.0), 300 mM KCl, and 20 mM imidazole (buffer A) with a flow rate of 2 mL/min. His-tagged protein E1 was eluted employing a linear imidazole gradient (from 0 to 100% buffer B) over 100 mL. The fractions containing E1 were pooled and concentrated to a final volume of 3 mL in microconcentrators (VIVASPIN 15R 30 kDa, 4000 rpm, 5 °C), washed with 15 mL of buffer containing 50 mM potassium phosphate (pH 7.0) and 300 mM KCl, and again concentrated to a volume of 3 mL. The concentrated solution was loaded onto a Superdex 75 gel filtration column at a flow rate of 1.5 mL/min. The fractions containing the E1 component were pooled again and concentrated in the manner described above in 100 mM potassium phosphate (pH 7.6) and 300 mM KCl. The purity of the protein was determined by SDS−PAGE, and the protein concentration was determined by absorbance using an extinction of 0.91 A_{280} mg^{-1} mL cm^{-1} for the apo-*hs*PDHc-E1 protein. The total amount of homogeneous protein varied between 17 and 25 mg. The protein was shock-frozen in liquid nitrogen and stored at −70 °C until it was used.

*Analytical Ultracentrifugation. Hs*PDHc-E1 was analyzed at initial protein concentrations of 0.02−1 mg/mL in 0.1 M potassium phosphate (pH 7.6), 0.3 M KCl, 1 mM $MgCl_2$, and 100 μM ThDP with a Beckman Optima XL-A centrifuge and an An50Ti rotor. Sedimentation equilibrium and sedimentation velocity measurements (absorption at 230 and 280 nm) were carried out in double-sector cells at 20 °C and 8000 and 40 000 rpm, respectively. Original data were analyzed with the software provided by Beckman Instruments (Palo Alto, CA). The dependence of the apparent sedimentation coefficient on the protein concentration was fitted to a dimer−tetramer equilibrium according to refs *17* and *18*.

Kinetic Single-Step Analysis of the E1-Only Reaction and H−D Exchange Kinetics at C2 of the Enzyme-Bound Cofactor by Rapid Quench−^{1}H NMR Spectroscopy. Apo-E1 (15.5 mg/mL, 201 μM active sites) was reconstituted with an equimolar amount of ThDP and 5 mM Mg^{2+} in 0.1 M potassium phosphate (pH 7.6) and 300 mM KCl at 30 °C for 5 min. The enzyme was mixed with a saturating concentration of pyruvate (50 mM) for defined reaction times in 0.1 M potassium phosphate (pH 7.6) and 300 mM KCl at 30 °C, either by using a rapid quench flow device (RQF-3, Kintek Althouse) for reaction times of up to 2000 ms or by manual mixing for longer reaction times. The reaction was quenched by the addition of 12.5% (w/v) TCA and 1 M DCl (in D_2O). The denatured protein was discarded after centrifugation, and the supernatant containing the intermediates and the substrate was analyzed by ^{1}H NMR spectroscopy. For the assignment and quantitative analysis of ThDP and covalent ThDP adducts, the C6′-H ^{1}H NMR signals of ThDP (8.01 ppm), LThDP (7.27 ppm), and HEThDP (7.33 ppm) were used. NMR acquisition and data processing were carried out as detailed in ref *15*. Kinetic analysis was performed as described in the Appendix.

The deprotonation rate constants at C2 of PDHc-E1-bound and free ThDP were determined using a H−D exchange technique as described in ref *14*. The apo-E1 enzyme (15.5 mg/mL) was reconstituted with ThDP and Mg^{2+} as described above and mixed with 1 volume of D_2O (99.9%) at 30 °C, by using a rapid quench flow device for reaction times of up to 2000 ms and by manual mixing for longer reaction times. After acid quench of the exchange reaction, the

Table 1: Kinetic and Thermodynamic Constants of *hs*PDHc-E1 in 0.1 M Potassium Phosphate (pH 7.6) and 0.3 M KCl at 30 °C

specific activity (milliunits/mg)[a]	60 ± 1
k_{cat} (s^{-1})[a]	0.077 ± 0.001
K_M(pyruvate) (μM)[a]	10.0 ± 1.5
K_D(ThDP) (μM)[b]	0.47 ± 0.08
K_D(methyl acetylphosphonate) (μM)[c]	46 ± 4
K_D(dimer−tetramer) (μM)	1.3 ± 0.1
ionization rate constant of C2 of ThDP, k_{obs} (s^{-1})[d]	51 ± 15 (activated site) 0.018 ± 0.005 (dormant site)
net rate constant of LThDP formation, k_1' (s^{-1})[d]	2.3 ± 0.5 (activated site) 0.029 ± 0.005 (dormant site)
net rate constant of LThDP decarboxylation, k_2' (s^{-1})[d]	5.1 ± 1.3 (activated site) $\gg k_1'$ (dormant site)

[a] The macroscopic kinetic constants were determined using the redox DCPIP assay (*16*). [b] The dissociation constant of ThDP was estimated by fluorescence titration experiments as detailed in ref *19*. [c] The apparent dissociation constant of the pyruvate analogue methyl acetylphosphonate was determined by circular dichroism spectroscopy as described in Materials and Methods. [d] The microscopic rate constants of elementary catalytic steps were determined by rapid quenched flow−^{1}H NMR spectroscopy as detailed in the text and refs *14* and *15*.

isolated cofactor was analyzed by ^{1}H NMR spectroscopy. The singlet signal of the C6′-H proton (8.01 ppm) was used as an internal nonexchanging standard. To obtain the exchange rates, the relative decay of the signal intensity of C2-H (9.68 ppm) was fitted to a monoexponential or multiexponential function as described in the Appendix.

Circular Dichroism Studies Using the Pyruvate Analogue Methyl Acetylphosphonate. The elusive 1′,4′-imino tautomer of the predecarboxylation intermediate analogue PLThDP formed upon covalent binding of the pyruvate analogue methyl acetylphosphonate to C2 of enzyme-bound ThDP was directly detected by CD spectroscopy (*10*). CD spectroscopic studies were carried out on a Jasco J-810 spectropolarimeter. For that purpose, *hs*PDHc-E1 (30 μM active sites) in 100 mM potassium phosphate (pH 7.6) and 300 mM KCl was reconstituted with ThDP (100 μM) and $MgSO_4$ (5 mM) for 10 min in a total volume of 150 μL. MAP as a sodium salt was diluted in the same buffer and titrated to the protein solution, yielding a final concentration of 1−8000 μM. CD spectra were recorded after a reaction time of 15 min in the 270−370 nm wavelength range at 20 °C. All spectra were corrected for buffer contributions. The apparent K_D for MAP was determined using eq 2:

$$\Theta_{(288-294)} = \frac{\Theta_{(288-294)max}[\mathrm{MAP}]}{K_D + [\mathrm{MAP}]} \qquad (2)$$

RESULTS

The recombinantly expressed and highly purified E1 component of *hs*PDHc exhibited kinetic constants similar to those described in related studies of other groups (*16*, *19*) with a specific activity of 60 milliunits/mg (corresponding to a k_{cat} of 0.077 s^{-1} per active site) at pH 7.6 and 30 °C in the DCPIP assay, an apparent K_M value for pyruvate of 10 μM, and a dissociation constant K_D for ThDP of 0.47 μM (Table 1). While using analytical ultracentrifugation (Figure 1), we can demonstrate that the heterotetramer is predominantly populated under the conditions (15 mg/mL enzyme) deployed for the kinetic NMR studies.

H−D Exchange Kinetics of C2-H of Enzyme-Bound ThDP in hPDHc-E1. The E1 component of *hs*PDHc is purified as

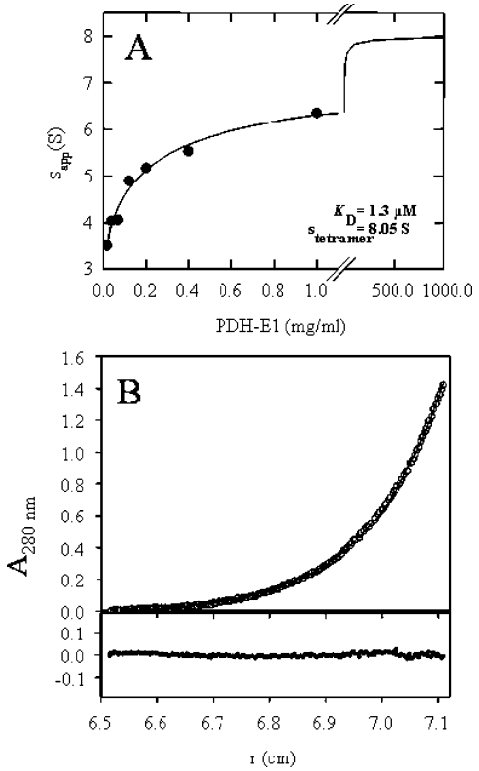

FIGURE 1: Association state of *hs*PDHc-E1. The association state of *hs*PDHc-E1 was analyzed by sedimentation velocity and sedimentation equilibrium at 20 °C using analytical ultracentrifugation. The protein was dissolved in 0.1 M potassium phosphate (pH 7.6), 0.3 M KCl, 1 mM $MgCl_2$, and 100 μM ThDP at protein concentrations of 0.02−1 mg/mL. (A) Sedimentation velocity was monitored at 40 000 rpm. The apparent *s* values (●) exhibited a dependence on the protein concentration that could be fitted (—) to a dimer−tetramer equilibrium with a dissociation constant K_D of 1.3 μM. (B) Sedimentation equilibrium of *hs*PDHc-E1 analyzed at a protein concentration of 1 mg/mL. The top panel displays the equilibrium data measured at 8 000 rpm and 20 °C (○) and the fit (—), and the bottom panel represents the deviation of the fit and data. The apparent molecular mass that was obtained was 141 kDa (mass of tetramer of ≈154 kDa), indicating a large fraction of the protein is tetrameric under these conditions.

an apoenzyme (sans ThDP and Mg^{2+}). Prior to the H−D exchange experiments, 15.5 mg/mL apo-E1 (corresponding to an active site concentration of 201 μM) was reconstituted with an equimolar amount of ThDP in the presence of 5 mM Mg^{2+}. Under these conditions, approximately 95% of all active sites are saturated with ThDP according to eqs A4 and A5 and the estimated K_D (ThDP) of 0.47 μM. As the total amplitude of the exchange reaction equals 0.5 due to 1:1 mixing and an isotope fractionation factor of C2-L (ThDP) being close to unity (see the Appendix), 95% of the observed amplitude (exchange amplitude = 0.475) reflects exchange of enzyme-bound ThDP (E−ThDP) and 5% (exchange amplitude = 0.025) corresponds to exchange of the free cofactor.

The analysis of the H−D exchange kinetics of holo-E1 revealed that approximately one-half of enzyme-bound ThDP exchanges within 2 s, whereas complete exchange in all active sites is accomplished after a reaction time of only 120 s (Figure 2). The estimated pseudo-first-order H−D exchange rate constant of the fast exchanging fraction ($k_{obs}^{E-ThDP1}$ = 51 ± 15 s^{-1}) and that of the less reactive fraction ($k_{obs}^{E-ThDP2}$ = 0.018 ± 0.005 s^{-1}) differ by more than 3 orders of magnitude (Figure 3). Surprisingly, ThDP bound to the

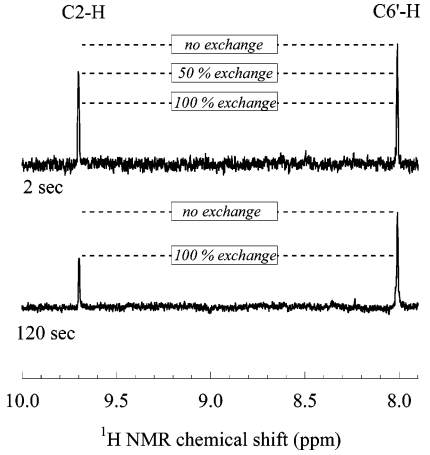

FIGURE 2: H−D exchange of C2-H of ThDP bound to *hs*PDHc-E1. Expansions of selected ^{1}H NMR spectra of acid quench isolated ThDP after reaction of 200 μL of 15.5 mg/mL holo-*hs*PDHc-E1 [in 0.1 M potassium phosphate (pH 7.6) and 300 mM KCl] with 200 μL of 99.9% D_2O for 2 s (top panel) and 120 s (bottom panel) at 30 °C displaying the ThDP signals of C2-H (9.70 ppm) and C6′-H (8.01 ppm) are shown. The latter signal serves as an internal nonexchanging standard for quantification.

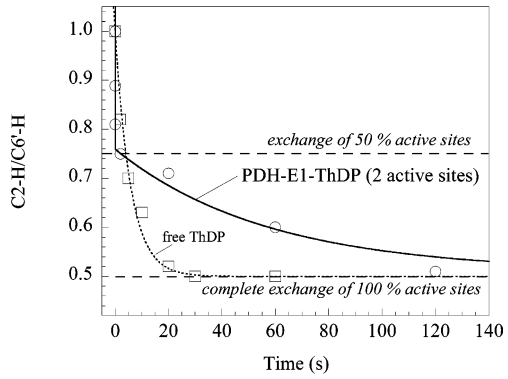

FIGURE 3: H−D exchange kinetics of free and *hs*PDHc-E1-bound ThDP in 0.1 M potassium phosphate (pH 7.6) and 300 mM KCl at 30 °C. The decay of the ^{1}H NMR integral intensity of ThDP's C2-H signal relative to the integral of the nonexchanging C6′-H signal was fitted to a monoexponential function for the free cofactor (□) or a double-exponential function for exchange of enzyme-bound ThDP (○) as detailed in the Appendix. The estimated pseudo-first-order rate constants are summarized in Table 1.

"inactive" site in E1 exchanges even 10 times slower than free cofactor ($k_{obs}^{ThDP} = 0.14 \pm 0.02$ s^{-1}) under identical conditions (Figure 3). This observation requires ThDP in the dormant site to be shielded from the solvent. The rate constant calculated for the active site is in the range of those reported for other thiamin enzymes (*14*, *20*). Notably, a half-of-the-sites reactivity in cofactor activation monitored by H−D exchange kinetics at C2 of ThDP has not been observed for any other thiamin enzyme so far.

Kinetic Analysis of the E1 Decarboxylation Reaction under Single-Turnover Conditions by Quench Flow−^{1}H NMR Spectroscopy. The decarboxylation reaction of the isolated E1 component of PDHc encompasses all steps up to and including decarboxylation of the 2-lactyl-ThDP intermediate (Scheme 1). The activity of the E1-only form in 2-ketoacid dehydrogenases is commonly monitored in a steady-state assay employing artificial electron acceptors such as 2,6-DCPIP that oxidize the HEThDP−enamine intermediate. An important caveat of this activity assay is that the kinetic significance of the artificial redox reaction and the subsequent hydrolysis of the formed 2-acyl-ThDP intermediate (2-acetyl-ThDP in PDHc-E1) for the overall reaction is unknown.

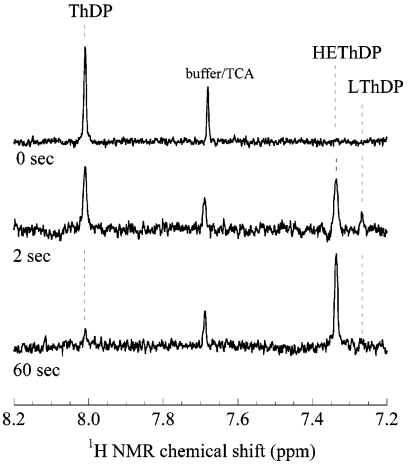

FIGURE 4: Distribution of covalent ThDP intermediates in the nonoxidative decarboxylation of pyruvate by *hs*PDHc-E1 under single-turnover conditions analyzed by ^{1}H NMR spectroscopy. The intermediates were isolated by acid quench after reaction of 15.5 mg/mL holo-*hs*PDHc-E1 with 50 mM pyruvate in 0.1 M potassium phosphate (pH 7.6) and 300 mM KCl at 30 °C for defined reaction times and were analyzed by ^{1}H NMR at pH 0.75 using the characteristic C6′-H chemical shifts of ThDP (8.01 ppm) and the covalent intermediates HEThDP (7.33 ppm) and LThDP (7.27 ppm) (*15*). The NMR spectra are a selection and display the intermediate distribution after reaction times of 0, 2, and 120 s.

Therefore, we examined the kinetics of the E1 reaction directly under single-turnover conditions with pyruvate at saturating amounts and analyzed the quantitative distribution of the reaction intermediates ThDP, LThDP, and HEThDP enamine using a chemical quench−^{1}H NMR spectroscopic method (*15*). As detailed in the Appendix, under these conditions, the unimolecular forward net rate constants of LThDP formation and decarboxylation can be assessed. In the course of the single-turnover reaction of E1 with pyruvate, the enzyme-bound ThDP is completely converted to HEThDP$^-$ with LThDP being an observable intermediate (Figure 4). The kinetic analysis of the time course of the different cofactor mole fractions (ThDP, LThDP, and HEThDP; see the Appendix) indicates a dynamic nonequivalence of the two active sites during pyruvate turnover. Approximately one-half of the active sites bind and decarboxylate pyruvate rapidly within 2 s. In the remaining 50% of the active sites in E1, the overall reaction is completed only after 60 s (Figure 4). Fitting the data (Figure 5 and Table 1) yielded two net rate constants for LThDP formation ($k_{1A}' = 2.3 \pm 0.5$ s^{-1}, and $k_{1B}' = 0.029 \pm 0.005$ s^{-1}) that differ by approximately 2 orders of magnitude. Noteworthy is the fact that the net rate constant of binding of covalent pyruvate to ThDP in the "inactive site" is in the range of the apparent C2 ionization rate constant of ThDP determined by H−D exchange experiments ($k_{obs}^2 = 0.018 \pm 0.005$ s^{-1}).

The transient nature of LThDP was directly confirmed by NMR spectroscopy (Figure 4), although this intermediate could be hardly detected because the maximum extent of its formation in the single-turnover reaction is very low (approximately 10% of the total active site concentration). The time course of its formation and decay was fitted to eq 8A and yielded rate constants of LThDP decarboxylation (k_{2A}') of 5.1 ± 1.3 s^{-1} in the activated center, and $k_{2B}' \gg k_{1B}'$ in

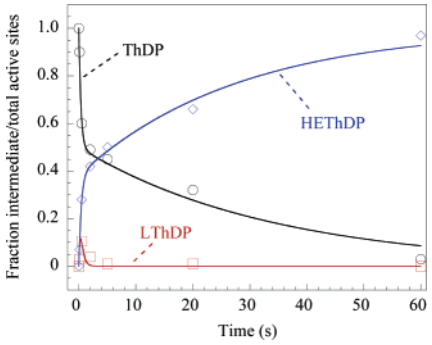

FIGURE 5: Kinetic analysis of the single-turnover reaction of *hs*PDHc-E1 with pyruvate. The relative mole fractions of ThDP (○), HEThDP (◇), and LThDP (□) at defined time points (compare to Figure 4) in the nonoxidative decarboxylation of pyruvate by *hs*PDHc-E1 were fitted to a consecutive reaction mechanism, taking into account half-of-the-sites reactivity as detailed in the Appendix (eqs A7−A9). The estimated net rate constants of LThDP formation (k_1') and LThDP decarboxylation (k_2') are summarized in Table 1.

the dormant site. Additional kinetic simulations (not shown) suggest that the observed LThDP fraction corresponds exclusively to the fast-working active site. When half-of-the-sites reactivity is taken into account, the maximum level of LThDP in the activated site is related to k_{1A}' (LThDP formation) and k_{2A}' (LThDP decarboxylation) as follows:

$$\frac{[\text{LThDP}]_{\max}}{[\text{active sites}]_{\text{total}}} = 0.5(k_{1A}'/k_{2A}')^{-k_{2A}'/(k_{1A}'-k_{2A}')} \quad (3)$$

Using this equation and the estimated net rate constants k_{1A}' and k_{2A}', the maximum extent of LThDP formation was calculated to account for 12% of all active sites which closely matches our experimental observation.

Circular Dichroism and ^{1}H NMR Studies of the Reaction of E1 with the Pyruvate Analogue Methyl Acetylphosphonate. Recent studies on model systems and bacterial PDHc-E1 suggested that the elusive 1′,4′-imino tautomer of the aminopyrimidine part of ThDP and ThDP intermediates gives rise to a positive CD signal centered at approximately 305 nm (*9*, *10*). Reconstitution of apo-E1 from *E. coli* with the stable LThDP analogue 2-phosphono-lactyl-ThDP (PLThDP) and Mg^{2+} results in the detectable formation of the imino tautomer which is suggested to be stabilized in the tetrahedral predecarboxylation intermediate analogue.

In our studies, we added the pyruvate analogue methyl acetylphosphonate (MAP) to human holo-PDHc-E1 rather than reconstituting the apoenzyme with the corresponding PLThDP adduct, which can be chemically synthesized as a racemic mixture only (*21*). While MAP is being added, a stereospecific formation of 1′,4′-imino-PLThDP in the enzyme is expected to take place (Scheme 2). The reaction of human E1 with MAP causes a positive CD signal centered around 290−305 nm (Figure 6A) similar to that observed for the bacterial enzyme. The apparent dissociation constant for MAP was estimated to be 46 ± 4 μM at pH 7.6 and 20 °C (Figure 6B). In addition to the CD spectroscopic studies which enable detection of the 1′,4′-imino tautomer of the aminopyrimidine ring, we quantitatively analyzed the formation of PLThDP, the covalent MAP−ThDP adduct, by ^{1}H NMR spectroscopy. These studies revealed that even after prolonged reaction times of 30 min at most only one-half of all active sites are occupied by PLThDP when MAP is added in saturating amounts (Figure 6C).

DISCUSSION

The minimal quaternary structure of ThDP enzymes known so far is that of a dimer or higher oligomeric states, such as tetramers. In all ThDP enzymes that have been structurally characterized so far, the cofactor is bound at the interface of two subunits forming a dimer (*6*, *22*−*33*). The questions of whether the two corresponding active sites in a dimer (i) exhibit similar reactivities in terms of a chemical equivalence and (ii) communicate with each other are longstanding ones. There have been instances where substrates in ThDP enzymes could induce a positive cooperativity of cofactor binding, indicating a communication of the active sites (*34*). Furthermore, kinetic turnover studies on some ThDP enzymes, such as pyruvate decarboxylase from yeast and benzoylformate decarboxylase, suggested the active sites do not work independently (*13*). However, the dynamic nonequivalence was inferred either from steady-state kinetics on a macroscopic kinetic scale or by making use of artificial substrates with endowed chromophores. Our understanding of these kinetic observations has been advanced by the determination of high-resolution structures of various thiamin enzymes, where in a few cases a structural nonequivalence of the two physically remote active sites in the dimer or pair of dimers has been observed (*11*, *31*). Most notably, in the crystal structure of a subcomplex formed between the $\alpha_2\beta_2$-type E1 subunit and the peripheral subunit-binding domain from the lipoate acetyltransferase (E2) of the *B. stearothermophilus* PDHc (*11*), several active site loops were found

Scheme 2: Reaction of Methyl Acetylphosphonate, a Phosphonate Analogue of Pyruvate, with *hs*PDHc-E1 Leads to the Formation of 1′,4′-Imino-2-α-phosphonolactyl-ThDP, a Stable LThDP Analogue

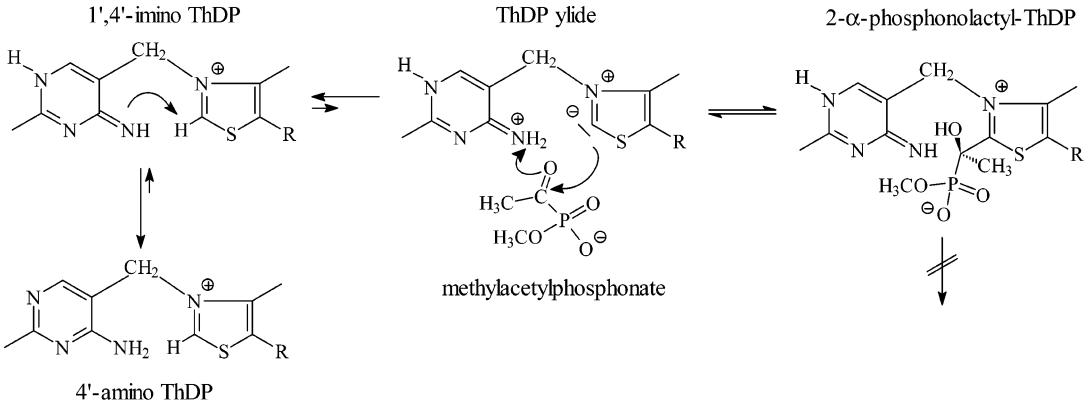

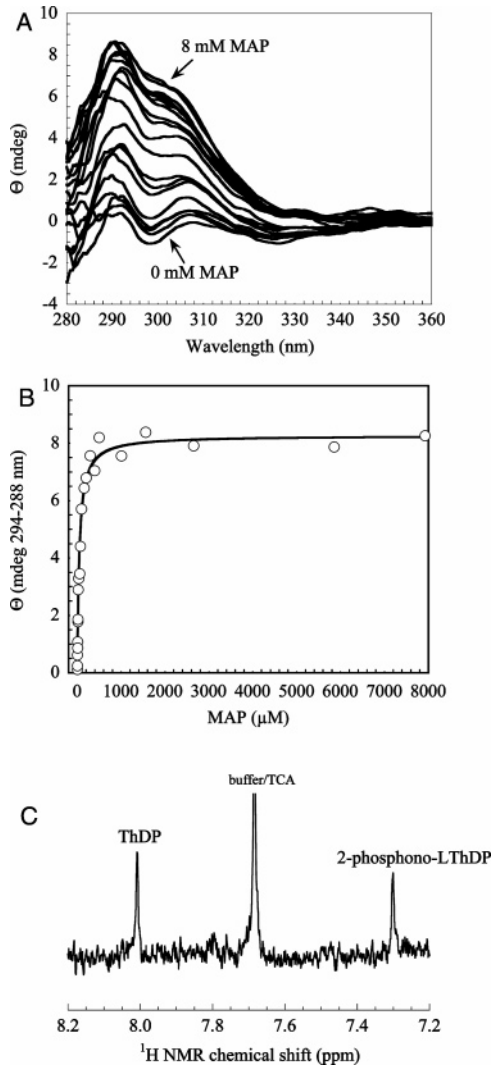

FIGURE 6: Formation of the stable LThDP analogue 1′,4′-imino-2α-phosphonolactyl-ThDP in *hs*PDHc-E1 after reaction of the enzyme with methyl acetylphosphonate as detected by circular dichroism and ^{1}H NMR spectroscopy. (A) Circular dichroism spectra obtained after addition of increasing amounts of the pyruvate analogue methyl acetylphosphonate (0−8 mM) to 30 μM holo-*hs*PDHc-E1 in 0.1 M potassium phosphate (pH 7.6) and 300 mM KCl at 20 °C. (B) Analysis of the dependence of the CD signal intensity at 288−294 nm on the MAP concentration was fitted to eq 2 and yielded a dissociation constant of 46 ± 4 μM. (C) Section of the ^{1}H NMR spectrum of acid quench isolated intermediates after reaction of 201 μM *hs*PDHc-E1 with 15 mM MAP in 0.1 M potassium phosphate (pH 7.6) and 300 mM KCl at 20 °C showing the C6′-H signals of unreacted ThDP (8.01 ppm) and PLThDP (7.30 ppm).

to be in an ordered state only in one of the two active sites. The detailed structural analysis of the subcomplex revealed that the N1 atom of ThDP in one active site is linked to N1′ of the other ThDP via an acidic tunnel consisting of Glu and Asp side chains and water molecules. This structural feature had been discovered in studies on transketolase at first (*35*) and appears to be common to many thiamin enzymes. The observation of an acidic tunnel between the remote active sites raises the possibility that it may be used for reversible charge (H^+) conduction as Schneider, Perham, and co-workers had discussed. Accordingly, protonation of N1′ of ThDP at one active site would trigger chemical activation of the cofactor, whereas the other active site would be in a dormant, nonactivated state with a deprotonated N1′. In the case of transketolase, the concept of an alternating activation state of ThDP at the two active sites can be ruled out because (i) both thiamin molecules in the dimer were found to be in an activated state exhibiting similar apparent C2 ionization rate constants (*14*) and (ii) both active sites are able to bind different donor substrates and substrate analogues at saturating concentrations with an active site occupancy close to unity as detected by X-ray crystallography (ref *36* and personal communication of G. Schneider) and NMR spectroscopy (*15*). As an alternative to the "proton wire" mechanism discussed above, a so-called "flip-flop" mechanism has been proposed to explain the suggested dynamic nonequivalence of the active site pairs in ThDP enzymes (*6*). Accordingly, the cofactors in the two active sites are chemically equivalent in the absence of the substrates, but chemical events in one active site such as LThDP formation trigger motions of domains making contacts with both active sites in the catalytic dimer and thus change the catalytic competence of the Glu−cofactor proton shuttle of the second site. As a consequence, the two active sites would also be in alternating phases of the catalytic cycle as suggested for the proton wire mechanism. The major difference between these two alternative mechanisms is that active center communication is intimately linked either to catalytic proton-transfer events with no major structural changes being necessary (proton wire mechanism) or to structural changes in the course of catalysis that switch the cofactor activation machinery of the corresponding subunit on and off (flip-flop mechanism).

How should one reliably detect a possible chemical and/or functional nonequivalence of active site pairs in ThDP enzymes and discriminate between a proton wire and a flip-flop mechanism? Although structural methods are valuable tools for detecting a structural nonequivalence, their use for the detection of a possible chemical and/or functional nonequivalence is subject to some restrictions. Even at atomic resolution, it will be challenging to differentiate between an activated and nonactivated ThDP cofactor in an enzyme, because cofactor activation appears to be controlled kinetically with the reactive C2 being protonated in the activated state, too (*14*, *37*). While using a H−D exchange technique, the activation state and chemical competence of the cofactor in the active site can be directly analyzed. For all enzymes that were studied so far in this regard, including pyruvate decarboxylase, transketolase, and pyruvate oxidase, all enzyme-bound cofactor molecules of a particular enzyme incorporated deuterium at C2 with the same apparent rate constant, suggesting a chemical equivalence of ThDP at both active sites in the absence of substrates (*14*, *20*). Our related studies on the human E1 component of PDHc presented in this study now provide the first example of a ThDP enzyme where a rapidly exchanging and a slowly exchanging fraction of enzyme-bound cofactor can be observed. As both fractions account for approximately 50% of active sites each, it may be concluded that, probably in dynamic equilibrium, one active site contains an activated cofactor and the other a nonactivated ThDP. Notably, in the X-ray crystal structure of *hs*PDHc-E1 determined at 1.95 Å (*6*), no structural differences between the two corresponding catalytic subunits of the tetramer were apparent, although they are nonequivalent in a chemical sense. Hence, there would be no need to invoke marked structural rearrangements in the course of

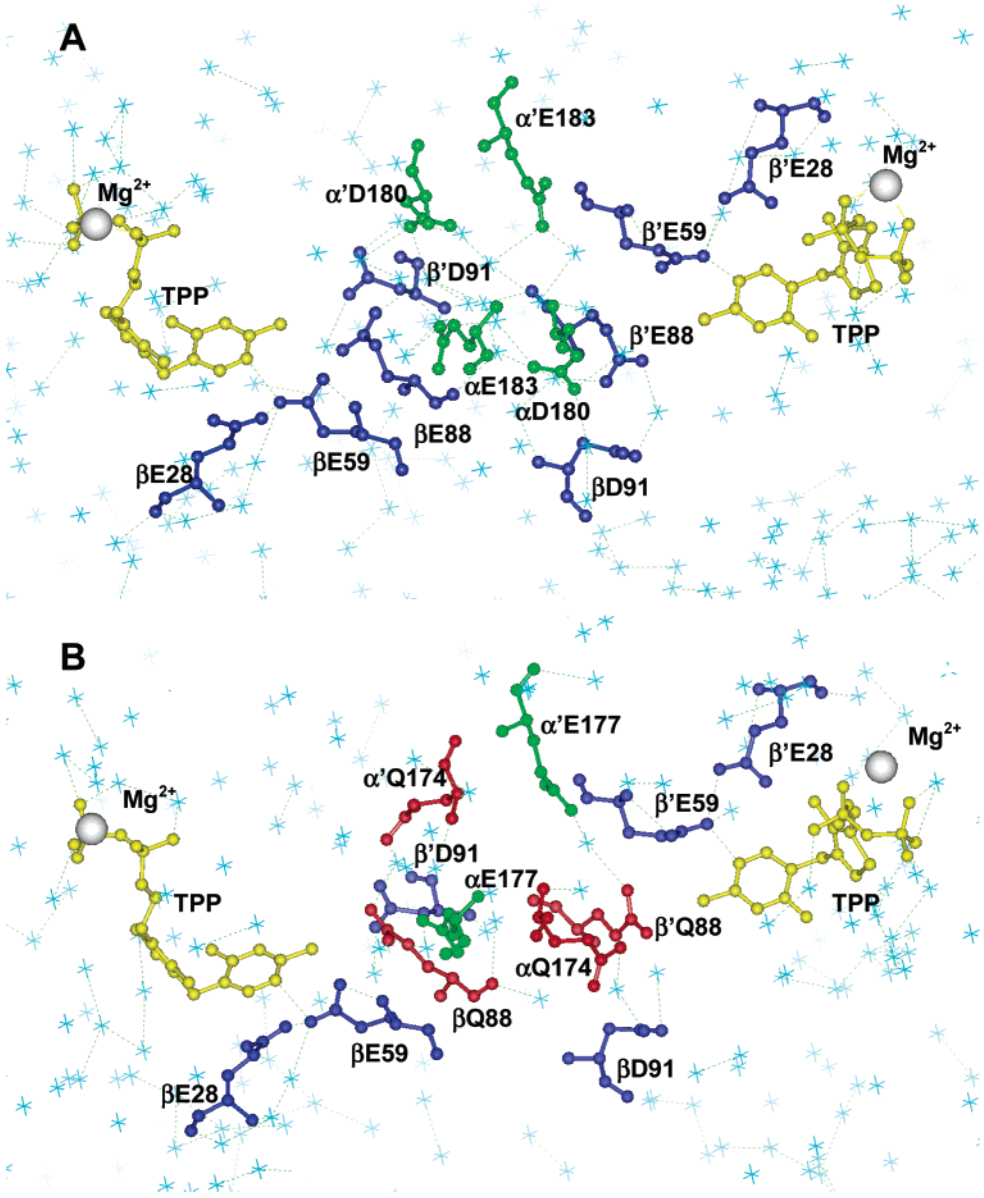

FIGURE 7: Comparison of the residues in the proton channel for *B. stearothermophilus* PDHc-E1 (A) and human PDHc-E1 (B). Only 12 negatively charged residues suggested to be involved in proton transfer are shown in the *B. stearothermophilus* E1 structure. The corresponding residues in the human E1 structure are displayed. The conserved residues of both *B. stearothermophilus* and human E1s in the α and α′ subunits are colored green and in the *β* and *β*′ subunits are colored dark blue. Four residues of 12 are replaced in human E1 and do not have a negative charge. These four residues in human E1 (in α, α′, *β*, and *β*′) are colored red. TPP is colored yellow, and Mg^{2+} ions are shown as white spheres. Hydrogen bonds are displayed. This figure has been created using InsightII and PDB entries 1NI4 and 1W85.

catalysis such as a flip-flop mechanism to explain the observed dynamic nonequivalence of the active sites. On the other hand, a flip-flop mechanism cannot be disapproved by the kinetic data and remains a viable alternative for the proton wire mechanism. At present, there is no ultimate proof to choose or decline either mechanism. An inspection of the X-ray structure of *hs*PDHc-E1 reveals that acidic side chains such as E59 and E177 are part of a hydrogen bonding network that links the two cofactors, presumably allowing for reversible charge conduction between the two remote sites (Figure 7). In contrast to E1 from *B. stearothermophilus*, not all side chains of the communication tunnel in human E1 are negatively charged.

As a consequence of the chemical nonequivalence, only one active site of E1 is able to bind the substrate analogue MAP to C2 of ThDP forming the predecarboxylation intermediate analogue PLThDP as detected by NMR and CD spectroscopy. Similar results were obtained when the enzyme was allowed to react with its physiological substrate pyruvate; only 50% of the active sites bind and decarboxylate pyruvate with a rate sufficient to account for catalysis of the E1-only form, whereas the dormant active site catalyzes the same sequence of reactions with a rate that is 2 orders of magnitude lower. The calculated net rate constant of LThDP formation of the dormant site at pyruvate saturation ($k' = 0.03\ s^{-1}$) is in the same range as the observed rate constant of cofactor activation ($k_{obs} = 0.02\ s^{-1}$), indicating that the slow formation of the reactive C2 carbanion of the nonactivated cofactor is rate-limiting for turnover at the dormant site. Contrary to our experiments with the substrate analogue MAP, we can detect covalent intermediates at the inactive site. This is very likely due to the quasi-irreversible decarboxylation of LThDP, which leads to a forward commitment of catalysis that cannot be attained when MAP is used. In the latter case,

the C_α−P bond of the formed PLThDP intermediate analogue cannot be cleaved enzymatically. Therefore, the absence of covalent intermediates suggests the off-rate of MAP at the inactive site to be markedly larger than the on-rate under the conditions used. In a joint study on the α_2-type PDHc-E1 from *E. coli* conducted with our collaborators from Rutgers University (Newark, NJ), we have also observed a functional nonequivalence of the active sites that cannot be detected in mutant proteins with exchanges of the conserved glutamate interacting with N1′ of ThDP (F. Jordan and K. Tittmann, unpublished results). Contrary to the results obtained on E1 from *hs*PDHc, we have no evidence for a functional nonequivalence of the two corresponding active sites in the related thiamin enzymes pyruvate decarboxylase (PDC) from *Zymomonas mobilis*, pyruvate oxidase (POX) from *Lactobacillus plantarum*, transketolase (TK) from *Saccharomyces cerevisiae*, and indolepyruvate decarboxylase (IPDC) from *Enterobacter cloacae*. If indeed a proton wire or a flip-flop mechanism was to synchronize the two active sites, one should, in theory, observe symmetric fractions of intermediates at the steady state of the enzymes, i.e., 50% of two distinct intermediates each. We have analyzed the intermediate distribution of these enzymes either at the true steady state (PDC, POX, and IPDC) or of the donor half-reaction (TK) by NMR spectroscopy. In neither case were symmetric (50%) populations of intermediates observed (*14*, *38*, *39*). This finding is not consistent with a half-of-the-sites reactivity in these enzymes but rather suggests the active sites to work independently. Furthermore, no structural changes of the active sites or of the putative communication tunnel are visible in X-ray crystallographic studies on catalytic intermediates in POX (*40*) and TK (*36*). The so far unique observed chemical and functional nonequivalence of the active sites in PDHc-E1 appears to be a special feature of pyruvate/2-ketoacid dehydrogenases. Why should PDHc-E1 synchronize the action of its active sites while other thiamin enzymes do not? A major difference between the enzymes mentioned above and PDHc-E1 is that only the latter is embedded in a highly organized and symmetric multienzyme complex. Structural studies on various intermediate analogues in bacterial PDHc-E1 provide evidence for large disorder-to-order transitions in the course of catalysis (*41*, *42*). It appears reasonable to hypothesize that the structural rearrangements not only accompany catalysis in E1 itself but also may trigger the reductive acetylation of E2 by E1. Thus, a synchronized mode of action in the two active sites of each E1 catalytic dimer would result in a synchronization of downstream events in E2 and E3. This overall synchronization may be a catalytic advantage in multienzyme complexes with a complex catalytic sequence involving several components.

Finally, the kinetic constants obtained for E1 of *hs*PDHc in this study allow us to draw some general conclusions. In view of the overall catalytic constant of the fully reconstituted PDH complex ($k_{cat} \approx 50-70\ s^{-1}$ per E1 active site at 30 °C and pH 7.6), the observed unimolecular net rate constants of LThDP formation ($k' = 2\ s^{-1}$) and decarboxylation ($k' = 5\ s^{-1}$) at the activated active site of isolated E1 under the same conditions cannot account for catalysis of E1 in the complex. Thus, full reactivity of E1 is accomplished only after its reconstitution with the E2, E3, and E3BP components in the complex. Furthermore, these results demonstrate that the catalytic constant of E1 obtained with the commonly used artificial DCPIP assay ($k_{cat} = 0.077\ s^{-1}$ at 30 °C) is severly smaller than those of all elementary catalytic steps of the E1-only reaction (cofactor activation, formation of the pyruvate·enzyme Michaelis complex, LThDP formation, and LThDP decarboxylation). This implies that the reaction of DCPIP with the HEThDP carbanion−enamine intermediate in E1 and the subsequent hydrolysis of the acetyl intermediate are almost completely rate-limiting for the artificial redox assay. This has to be kept in mind when interpreting kinetic steady-state data of thiamin-dependent E1 components of 2-ketoacid multienzyme complexes using artificial electron acceptors.

APPENDIX

H−D Exchange Kinetics of the Reactive C2-H of Free and Enzyme-Bound ThDP. Mixing of free ThDP or ThDP-containing enzymes in aqueous (H_2O) buffer with D_2O results in the incorporation of deuterium at C2 of ThDP until an equilibrium with constant fractions of C2-H and C2-D is established. The equilibrium position depends on the mole fraction of deuterium after mixing denoted as n_D, and the isotopic fractionation factor Φ_{C2-L} of the acidic C2 of ThDP. In these studies, a 1:1 mixing ratio was adjusted throughout all H−D exchange experiments, resulting in an n_D of 0.5. The isotopic fractionation factor Φ_{C2-L} is defined as

$$\Phi_{C2-L} = \frac{X_{C2-D}}{X_{C2-H}} \frac{1 - n_D}{n_D} \tag{A1}$$

where X represents the mole fraction of either C2-D or C2-H. The isotopic fractionation factors of C2-L of both free and enzyme-bound ThDP in various enzymes are close to unity (*43*, *44*) and can therefore be neglected in the analysis.

The H−D exchange reaction can be kinetically treated as a pseudo-first-order reaction which follows a single-exponential function:

$$\frac{\int \text{C2-H}}{\int \text{C6′-H}}(t) = n_D \frac{\int \text{C2-H}}{\int \text{C6′-H}}(t_0) \times \exp(-k_{obs} t) + (1 - n_D) \tag{A2}$$

where $\int$C2-H is the relative ^{1}H NMR integral of the exchanging C2-H and $\int$C6′-H that of the nonexchanging C6′-H as an internal standard. At t_0, the ratio of both is 1.

When the H−D exchange of a ThDP-dependent enzyme with a reversibly binding cofactor is kinetically analyzed, the fractions of both bound and free cofactor in equilibrium have to be taken into account. The fraction of enzyme-bound ThDP (E−ThDP) and free cofactor (ThDP) can be estimated according to eqs A3 and A4, respectively:

$$[\text{E−ThDP}] = \frac{[\text{ThDP}]_0 + [\text{E}]_0 + K_D}{2} - \sqrt{\frac{([\text{ThDP}]_0 + [\text{E}]_0 + K_D)^2}{4} - [\text{ThDP}]_0[\text{E}]_0} \tag{A3}$$

$$[\text{ThDP}] = [\text{ThDP}]_0 - [\text{E−ThDP}] \tag{A4}$$

where $[E]_0$ is the total active site concentration and K_D the dissociation constant of ThDP.

Considering a chemical nonequivalence of the two active sites in PDHc-E1, the H−D exchange kinetics may consist of as many as three phases, two of which reflect exchange at the two different active sites (E−ThDP1 and E−ThDP2) and one of which reflects exchange of free ThDP.

$$\frac{\int \text{C2-H}}{\int \text{C6}'\text{-H}}(t) = n_D \frac{\int \text{C2-H}}{\int \text{C6}'\text{-H}}(t_0)\left[\frac{0.5[\text{E}-\text{ThDP}]}{[\text{E}-\text{ThDP}]+[\text{ThDP}]} \times \exp(-k_{\text{obs}}^{\text{E}-\text{ThDP1}} t) + \frac{0.5[\text{E}-\text{ThDP}]}{[\text{E}-\text{ThDP}]+[\text{ThDP}]} \times \exp(-k_{\text{obs}}^{\text{E}-\text{ThDP2}} t) + \frac{[\text{ThDP}]}{[\text{E}-\text{ThDP}]+[\text{ThDP}]} \times \exp(-k_{\text{obs}}^{\text{ThDP}} t)\right] + (1 - n_D) \quad \text{(A5)}$$

Notably, the relative exchange amplitudes for E−ThDP1 and E−ThDP2 should be 50% each of that of E−ThDP (total) if a half-of-the-sites mechamism applies for the enzyme. When the fraction of free cofactor is negligible, the third exponential term in eq A5 can be omitted.

Kinetic Analysis of the Single-Turnover Experiments of E1 with Pyruvate. When E1 alone is reacted with pyruvate, only a single turnover takes place, yielding the HEThDP carbanion−enamine form as the final intermediate (see Scheme 1). At pyruvate saturation, the rate of this reaction is kinetically determined by the ligation of pyruvate held in a docking site to C2 of ThDP (k_1') and the decarboxylation of the formed LThDP intermediate (k_2').

$$\text{E}-\text{ThDP} + \text{pyruvate} \Leftrightarrow \text{E}-\text{ThDP}\cdot\text{pyruvate} \xrightarrow{k_1'} \text{E}-\text{LThDP} \xrightarrow{k_2'} \text{E}-\text{HEThDP}^- + \text{CO}_2 \quad \text{(A6)}$$

The mole fractions of E−ThDP, E−LThDP, and E−HEThDP at any time point of the reaction can be related to k_1' and k_2' according to eqs A7−A9, and taking into account a different reactivity of the two active sites in E1:

$$[\text{E}-\text{ThDP}](t) = 0.5[\text{E}-\text{ThDP}]_0 \times \exp(-k_{1\text{A}}' t) + 0.5[\text{E}-\text{ThDP}]_0 \times \exp(-k_{1\text{B}}' t) \quad \text{(A7)}$$

$$[\text{E}-\text{LThDP}](t) = 0.5[\text{E}-\text{ThDP}]_0 \frac{k_{1\text{A}}'}{k_{2\text{A}}' - k_{1\text{A}}'} \times [\exp(-k_{1\text{A}}' t) - \exp(-k_{2\text{A}}' t)] + 0.5[\text{E}-\text{ThDP}]_0 \frac{k_{1\text{B}}'}{k_{2\text{B}}' - k_{1\text{B}}'} \times [\exp(-k_{1\text{B}}' t) - \exp(-k_{2\text{B}}' t)] \quad \text{(A8)}$$

$$[\text{E}-\text{HEThDP}^-](t) = 0.5[\text{E}-\text{ThDP}]_0\left[1 + \frac{k_{1\text{A}}' \exp(-k_{2\text{A}}' t) - k_{2\text{A}}' \exp(-k_{1\text{A}}' t)}{k_{2\text{A}}' - k_{1\text{A}}'}\right] + 0.5[\text{E}-\text{ThDP}]_0\left[1 + \frac{k_{1\text{B}}' \exp(-k_{2\text{B}}' t) - k_{2\text{B}}' \exp(-k_{1\text{B}}' t)}{k_{2\text{B}}' - k_{1\text{B}}'}\right] \quad \text{(A9)}$$

The time course of [E−ThDP] was fitted according to eq A7, thereby yielding estimates of the forward net rate constants k_1' (C−C ligation) in both active sites ($k_{1\text{A}}'$ and $k_{1\text{B}}'$). These rate constants were used to fit [E−LThDP](t) and [E−HEThDP](t) to eqs A8 and A9 to calculate $k_{2\text{A}}'$ and $k_{2\text{B}}'$, respectively (decarboxylation of LThDP).

ACKNOWLEDGMENT

We thank Rainer Rudolph for generous access to the fermentation facilities in the Institut für Biotechnologie and Gunter Schneider and Gerhard Hübner for stimulating discussions.

REFERENCES

1. Patel, M. S., and Roche, T. E. (1990) Molecular biology and biochemistry of pyruvate dehydrogenase complexes, *FASEB J. 4*, 3224−3233.
2. Korotchkina, L. G., and Patel, M. S. (2001) Probing the mechanism of inactivation of human pyruvate dehydrogenase by phosphorylation of three sites, *J. Biol. Chem. 276*, 5731−5738.
3. Korotchkina, L. G., and Patel, M. S. (2001) Site specificity of four pyruvate dehydrogenase kinase isoenzymes toward the three phosphorylation sites of human pyruvate dehydrogenase, *J. Biol. Chem. 276*, 37223−37229.
4. Roche, T. E., Baker, J. C., Yan, X., Hiromasa, Y., Gong, X., Peng, T., Dong, J., Turkan, A., and Kasten, S. A. (2001) Distinct regulatory properties of pyruvate dehydrogenase kinase and phosphatase isoforms, *Prog. Nucleic Acid Res. Mol. Biol. 70*, 33−75.
5. Gruys, K. J., Datta, A., and Frey, P. A. (1989) 2-Acetylthiamin pyrophosphate (acetyl-TPP) pH-rate profile for hydrolysis of acetyl-TPP and isolation of acetyl-TPP as a transient species in pyruvate dehydrogenase catalyzed reactions, *Biochemistry 28*, 9071−9080.
6. Ciszak, E. M., Korotchkina, L. G., Dominiak, P. M., Sidhu, S., and Patel, M. S. (2003) Structural basis for flip-flop action of thiamin pyrophosphate-dependent enzymes revealed by human pyruvate dehydrogenase, *J. Biol. Chem. 278*, 21240−21246.
7. Khailova, L. S., and Korochkina, L. G. (1985) Half-of-the-site reactivity of the decarboxylating component of the pyruvate dehydrogenase complex from pigeon breast muscle with respect to 2-hydroxyethyl thiamine pyrophosphate, *Biochem. Int. 11*, 509−516.
8. Khailova, L. S., Korochkina, L. G., and Severin, S. E. (1990) Intersite cooperativity in enzyme action of pyruvate dehydrogenase, in *Biochemistry and Physiology of Thiamin Diphosphate Enzymes* (Bisswanger, H., and Ullrich, J., Eds.) pp. 251−265, VCH Weinheim, Blaubeuren, Germany.
9. Jordan, F., Nemeria, N. S., Zhang, S., Yan, Y., Arjunan, P., and Furey, W. (2003) Dual catalytic apparatus of the thiamin diphosphate coenzyme: Acid-base via the 1,4′-iminopyrimidine tautomer along with its electrophilic role, *J. Am. Chem. Soc. 125*, 12732−12738.
10. Nemeria, N., Baykal, A., Joseph, E., Zhang, S., Yan, Y., Furey, W., and Jordan, F. (2004) Tetrahedral intermediates in thiamin diphosphate-dependent decarboxylations exist as a 1′,4′-imino tautomeric form of the coenzyme, unlike the michaelis complex or the free coenzyme, *Biochemistry 43*, 6565−6575.
11. Frank, R. A., Titman, C. M., Pratap, J. V., Luisi, B. F., and Perham, R. N. (2004) A molecular switch and proton wire synchronize the active sites in thiamine enzymes, *Science 306*, 872−876.
12. Jordan, F. (2004) How active sites communicate in thiamine enzymes, *Science 306*, 818−820.
13. Jordan, F., Nemeria, N. S., and Sergienko, E. (2005) Multiple modes of active center communication in thiamin diphosphate-dependent enzymes, *Acc. Chem. Res. 38*, 755−763.
14. Kern, D., Kern, G., Neef, H., Tittmann, K., Killenberg-Jabs, M., Wikner, C., Schneider, G., and Hübner, G. (1997) How thiamine diphosphate is activated in enzymes, *Science 275*, 67−70.
15. Tittmann, K., Golbik, R., Uhlemann, K., Khailova, L., Schneider, G., Patel, M. S., Jordan, F., Chipman, D. M., Duggleby, R. G., and Hübner, G. (2003) NMR analysis of covalent intermediates in thiamin diphosphate enzymes, *Biochemistry 42*, 7885−7891.
16. Korotchkina, L. G., Tucker, M. M., Thekkumkara, T. J., Madhusudhan, K. T., Pons, G., Kim, H. J., and Patel, M. S. (1995) Overexpression and Characterization of Human Tetrameric Pyruvate Dehydrogenase and Its Individual Subunits, *Protein Expression Purif. 6*, 79−90.

17. Hesterberg, L. K., and Lee, J. C. (1981) Self-association of rabbit muscle phosphofructokinase at pH 7.0: Stoichiometry, *Biochemistry 20*, 2974−2980.
18. Luther, M. A., Cai, G., and Lee, J. C. (1986) Thermodynamics of dimer and tetramer formations in rabbit muscle phosphofructokinase, *Biochemistry 25*, 7931−7937.
19. Fang, R., Nixon, P. F., and Duggleby, R. G. (1998) Identification of the catalytic glutamate in the E1 component of human pyruvate dehydrogenase, *FEBS Lett. 437*, 273−277.
20. Hübner, G., Tittmann, K., Killenberg-Jabs, M., Schäffner, J., Spinka, M., Neef, H., Kern, D., Kern, G., Schneider, G., Wikner, C., and Ghisla, S. (1998) Activation of thiamin diphosphate in enzymes, *Biochim. Biophys. Acta 1385*, 221−228.
21. Kluger, R., and Pike, D. C. (1977) Active site generated analogs of reactive intermediates in enzymic reactions. Potent inhibition of pyruvate dehydrogenase by a phosphonate analog of pyruvate, *J. Am. Chem. Soc. 99*, 4505−4506.
22. Lindqvist, Y., Schneider, G., Ermler, U., and Sundström, M. (1992) Three-dimensional structure of transketolase, a thiamine diphosphate dependent enzyme, at 2.5 Å resolution, *EMBO J. 11*, 2373−2379.
23. Muller, Y. A., and Schulz, G. E. (1993) Structure of the thiamine- and flavin-dependent enzyme pyruvate oxidase, *Science 259*, 965−967.
24. Pang, S. S., Duggleby, R. G., and Guddat, L. W. (2002) Crystal structure of the catalytic subunit of yeast acetohydroxyacid synthase: A target for herbidical inhibitors, *J. Mol. Biol. 317*, 249−262.
25. Arjunan, P., Umland, T., Dyda, F., Swaminathan, S., Furey, W., Sax, M., Farrenkopf, B., Gao, Y., Zhang, D., and Jordan, F. (1996) Crystal structure of the thiamine diphosphate-dependent enzyme pyruvate decarboxylase from the yeast *Saccharomyces cerevisiae* at 2.3 Å resolution, *J. Mol. Biol. 256*, 590−600.
26. Arjunan, P., Nemeria, N., Brunskill, A., Chandrasekhar, K., Sax, M., Yan, Y., Jordan, F., Guest, J. R., and Furey, W. (2002) Structure of the pyruvate dehydrogenase multienzyme complex E1 component from *Escherichia coli* at 1.85 Å resolution, *Biochemistry 41*, 5213−5221.
27. Chabriere, E., Charon, M. H., Volbeda, A., Pieulle, L., Hatchikian, E. C., and Fontecilla-Camps, J. C. (1999) Crystal structures of the key anaerobic enzyme pyruvate:ferredoxin oxidoreductase, free and in complex with pyruvate, *Nat. Struct. Biol. 6*, 182−190.
28. Hasson, M. S., Muscate, A., McLeish, M. J., Polovnikova, L. S., Gerlt, J. A., Kenyon, G. L., Petsko, G. A., and Ringe, D. (1998) The crystal structure of benzoylformate decarboxylase at 1.6 Å resolution: Diversity of catalytic residues in thiamin diphosphate-dependent enzymes, *Biochemistry 37*, 9918−9930.
29. Dobritzsch, D., König, S., Schneider, G., and Lu, G. (1998) High resolution crystal structure of pyruvate decarboxylase from *Zymomonas mobilis*. Implications for substrate activation in pyruvate decarboxylases, *J. Biol. Chem. 273*, 20196−20204.
30. Schütz, A., Sandalova, T., Ricagno, S., Hübner, G., König, S., and Schneider, G. (2003) Crystal structure of thiamindiphosphate-dependent indolepyruvate decarboxylase from *Enterobacter cloacae*, an enzyme involved in the biosynthesis of the plant hormone indole-3-acetic acid, *Eur. J. Biochem. 270*, 2312−2321.
31. Nakai, T., Nakagawa, N., Maoka, N., Masui, R., Kuramitsu, S., and Kamiya, N. (2004) Ligand-induced conformational changes and a reaction intermediate in branched-chain 2-oxo acid dehydrogenase (E1) from *Thermus thermophilus* HB8, as revealed by X-ray crystallography, *J. Mol. Biol. 337*, 1011−1033.
32. Mosbacher, T. G., Müller, M., and Schulz, G. E. (2005) Structure and mechanism of the ThDP-dependent benzaldehyde lyase from *Pseudomonas fluorescens*, *FEBS Lett. 272*, 6067−6076.
33. Machius, M., Wynn, R. M., Chuang, J. L., Li, J., Kluger, R., Yu, D., Tomchick, D. R., Brautigam, C. A., and Chuang, D. T. (2006) A versatile conformational switch regulates reactivity in human branched-chain α-ketoacid dehydrogenase, *Structure 14*, 287−298.
34. Horn, F., and Bisswanger, H. (1983) Regulatory properties of the pyruvate dehydrogenase complex from *Escherichia coli*. Studies on the thiamin diphosphate-dependent lag phase, *J. Biol. Chem. 258*, 6912−6919.
35. Nikkola, M., Lindqvist, Y., and Schneider, G. (1994) Refined structure of transketolase from *Saccharomyces cerevisiae* at 2.0 Å resolution, *J. Mol. Biol. 238*, 387−404.
36. Fiedler, E., Thorell, S., Sandalova, T., Golbik, R., König, S., and Schneider, G. (2002) Snapshot of a key intermediate in enzymatic thiamin catalysis: Crystal structure of the α-carbanion of (α,β-dihydroxyethyl)-thiamin diphosphate in the active site of transketolase from *Saccharomyces cerevisiae*, *Proc. Natl. Acad. Sci. U.S.A. 99*, 591−595.
37. Tittmann, K., Neef, H., Golbik, R., Hübner, G., and Kern, D. (2005) Kinetic control of thiamin diphosphate activation in enzymes studied by proton-nitrogen correlated NMR spectroscopy, *Biochemistry 44*, 8697−8700.
38. Schütz, A., Golbik, R., König, S., Hübner, G., and Tittmann, K. (2005) Intermediates and transition states in thiamin diphosphate-dependent decarboxylases. A kinetic and NMR study on wild-type indolepyruvate decarboxylase and variants using indolepyruvate, benzoylformate, and pyruvate as substrates, *Biochemistry 44*, 6164−6179.
39. Tittmann, K., Wille, G., Golbik, R., Weidner, A., Ghisla, S., and Hübner, G. (2005) Radical phosphate transfer mechanism for the thiamin diphosphate- and FAD-dependent pyruvate oxidase from *Lactobacillus plantarum*. Kinetic coupling of intercofactor electron transfer with phosphate transfer to acetyl-thiamin diphosphate via a transient FAD semiquinone/hydroxyethyl-ThDP radical pair, *Biochemistry 44*, 13291−13303.
40. Wille, G., Meyer, D., Steinmetz, A., Hinze, E., Golbik, R., and Tittmann, K. (2006) The catalytic cycle of a thiamin diphosphate enzyme examined by cryocrystallography, *Nat. Chem. Biol. 2*, 324−328.
41. Arjunan, P., Sax, M., Brunskill, A., Chandrasekhar, K., Nemeria, N., Zhang, S., Jordan, F., and Furey, W. (2006) A thiamin-bound, pre-decarboxylation reaction intermediate analogue in the pyruvate dehydrogenase E1 subunit induces large scale disorder-to-order transformations in the enzyme and reveals novel structural features in the covalently bound adduct, *J. Biol. Chem. 281*, 15296−15303.
42. Arjunan, P., Chandrasekhar, K., Sax, M., Brunskill, A., Nemeria, N., Jordan, F., and Furey, W. (2004) Structural determinants of enzyme binding affinity: The E1 component of pyruvate dehydrogenase from *Escherichia coli* in complex with the inhibitor thiamin thiazolone diphosphate, *Biochemistry 43*, 2405−2411.
43. Harris, T. K., and Washabaugh, M. W. (1995) Solvent-derived protons in catalysis by brewers' yeast pyruvate decarboxylase, *Biochemistry 34*, 14001−14011.
44. Tittmann, K. (2000) Ph.D. Thesis, Martin-Luther-University Halle-Wittenberg, Halle/Saale, Germany.

BI061582L